

# 2,8-Dihalogenated Diazocines: Versatile Reactants for Functionalized Photoswitches

Maximilian J. Notheis<sup>✉</sup>Vigan Sahiti<sup>✉</sup>

Vivienne Prangenberg

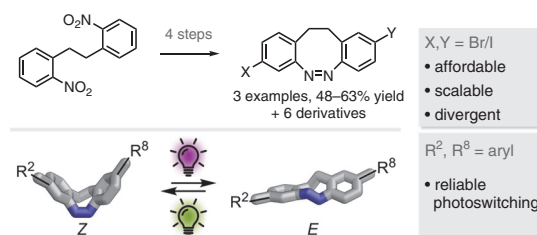
Johannes S. Kruse

Larissa K. S. von Krbek<sup>\*</sup>

Kekulé-Institut für Organische Chemie und Biochemie, Rheinische Friedrich-Wilhelms-Universität Bonn, Gerhard-Domagk-Str. 1, 53121 Bonn, Germany  
larissa.vonkrbek@uni-bonn.de

<sup>✉</sup> These authors contributed equally

Published as part of the Cluster Supramolecular Catalysis and Molecular Switches



Received: 25.02.2025

Accepted after revision: 21.03.2025

Published online: 26.03.2025 (Accepted Manuscript),

12.05.2025 (Version of Record)

DOI: 10.1055/a-2567-1399; Art ID: ST-2025-02-0095-L

License terms:



© 2025. The Author(s). This is an open access article published by Thieme under the terms of the Creative Commons Attribution License, permitting unrestricted use, distribution and reproduction, so long as the original work is properly cited. (<https://creativecommons.org/licenses/by/4.0/>)

**Abstract** Diazocine photoswitches possess distinctive structural characteristics and remarkable photochemical properties, leading to their growing application in photopharmacology and smart materials. We report the synthesis of 2,8-pseudo-*para*-substituted diazocines with two bromo, two iodo, or a combination of both substituents, achieving effective scalability. Besides demonstrating good reactivity in Suzuki cross-coupling reactions, the substituted diazocines predominantly retain their good photochemical properties, rendering them valuable components for said applications.

**Key words** photoswitches, diazocines, cross-coupling, gram-scale synthesis, photophysical properties

Ethylene-bridged azobenzene derivatives, termed diazocines, exhibit remarkable photoconversion between the thermodynamically stable U-shaped *Z*-isomer and the pseudo-planar metastable *E*-isomer (Figure 1), achieving photostationary states up to 92% (*E*),<sup>1</sup> and excellent quantum yields ranging from 70 to 90%.<sup>2</sup> The distinctive features of diazocines, combined with their ability to undergo visible-light photoswitching, have sparked significant interest in potential applications such as photodynamic therapy,<sup>3–6</sup> molecular imaging,<sup>7</sup> optical data storage,<sup>8</sup> and photoreponsive polymers.<sup>7–12</sup>

A diverse range of potential applications calls for various diazocine substitution patterns focusing on their ability to participate in efficient late-stage functionalizations, for example, in cross-coupling reactions.<sup>2,4</sup> Pseudo-*meta* substitutions in the 2,9- and 3,8-positions are the most common substitution patterns in diazocines (Figure 1a, **B** and

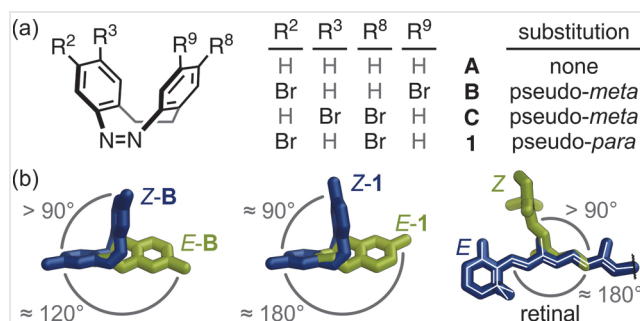
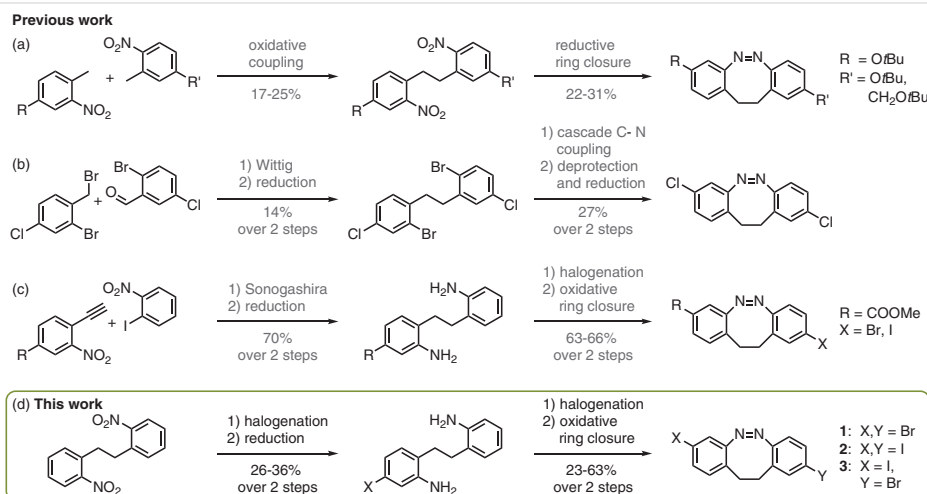


**Figure 1** (a) Reported examples of pseudo-*meta*-dibromo diazocines (**B** and **C**)<sup>2,6</sup> and our pseudo-*para*-dibromo diazocine **1**. (b) A structural comparison of the *E*- and *Z*-isomers of **B**, **1**, and retinal, respectively, illustrating the unique near-180° angle between the two substituents in *E*-1 [thermodynamically stable isomers: blue; metastable isomers: green]. GFN2-xTB<sup>13</sup> structures (diazocines: Supplementary Information, Section S8) and crystal structures<sup>14,15</sup> (retinal)]

**C**).<sup>3,7–9,12</sup> Conversely, pseudo-*para* substitution at the 2,8-positions of diazocines (**1**) remains uncommon, primarily because of synthetic difficulties arising from the asymmetric substitution pattern. This is despite a significantly greater change in distance and angle between the two substituents during photoisomerization (from 90° to 180°) compared with their pseudo-*meta* analogues (from 90° to 120°; Figure 1b), which is typically advantageous for many applications of photoswitches. This considerable change in the angle of the substituents is akin to the structural differences between *E*- and *Z*-retinal, which Nature employs in rhodopsin to efficiently convert light into a chemical signal in the eye (Figure 1b; right). For the employment of diazocines in various cross-coupling reactions, introducing halide substituents, preferentially bromides and iodides, is essential. However, this remains a challenge for 2,8-pseudo-*para*-substituted diazocines.<sup>2,4</sup>

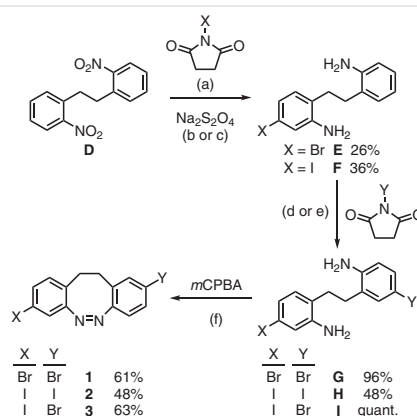


**Scheme 1** Previous syntheses of 2,8-disubstituted diazocines by (a) Herges and co-workers,<sup>3</sup> (b) Staubitz and co-workers,<sup>18</sup> and (c) Trauner and co-workers.<sup>2</sup> (d) Our approach.

Several 2,8-pseudo-*para*-substituted diazocines have been synthesized from asymmetrically substituted ethylene-bridged precursors by a ring-closing step that involves reducing dinitro derivatives,<sup>3,16</sup> the oxidation of dianiline compounds,<sup>2,17</sup> or a cross-coupling strategy involving a diiodide precursor<sup>18</sup> [Scheme 1; see also the Supporting Information (SI), Section S7]. This asymmetric ethylene-bridged precursor had previously been obtained by three different strategies. The first strategy involved statistical coupling of two nitrotoluene derivatives to form an isomeric mixture of the corresponding 2,2'-dinitrodibenzyl derivative,<sup>3</sup> separation of which was nontrivial, particularly when halide substituents were involved. The diazocine was formed through reductive ring closure. In the second strategy, a Wittig reaction was followed by double-bond reduction and a bromine-to-iodine halide exchange to permit diazocine formation through a cross-coupling strategy.<sup>18</sup> Because halide substituents are essential for forming the diazocine, this approach cannot yield diazocines with bromide or iodide substituents. Thirdly, a Sonogashira cross-coupling reaction followed by the reduction of the triple bond with hydrogen and Pd on charcoal gave a monosubstituted asymmetric precursor. A second substituent was selectively introduced onto the ethylene-bridged dianiline precursor, which subsequently underwent oxidative ring closure to yield the diazocine.<sup>2</sup> The initial substituent had to remain unaffected by the reduction conditions, which ruled out iodo and bromo substituents. Given the challenges posed by these synthetic routes for bromo and iodo substituents, alternative pathways needed to be explored for 2,8-pseudo-*para*-halide-substituted diazocines.

Here, we report the synthesis of 2,8-pseudo-*para*-substituted diazocines with two bromo, two iodo, or a combination of the two substituents (**1**, **2**, and **3**, respectively) by harnessing the different regioselectivities of electron-defi-

cient 2,2'-dinitrodibenzyl and electron-rich 2,2'-diaminodibenzyl toward aromatic halogenations (Scheme 2). Subsequently, we demonstrated the ability of diiodo diazocine **2** to undergo Suzuki cross-coupling reactions, introducing a diverse range of aryl substituents with various electronic properties (ranging from electron-rich to electron-deficient) onto the diazocine scaffold. The bromo iodo diazocine **3** was successfully used to sequentially introduce two distinct substituents featuring opposing electronic characteristics: one electron-rich and the other electron-deficient. The photophysical properties of all the diazocine derivatives were examined.



**Scheme 2** Synthesis of 2,8-pseudo-*para*-halogenated diazocines **1**, **2**, and **3** from commercially available 2,2'-dinitrodibenzyl (**D**). **Reaction conditions:** (a) NBS or NIS (1.1 equiv), concd H<sub>2</sub>SO<sub>4</sub>, r.t., 1 d or 1 h, **D** (1.84 or 40.0 mmol, respectively); (b) Na<sub>2</sub>S<sub>2</sub>O<sub>4</sub> (8 equiv), 1:1 (v/v) 1,4-dioxane–water, 120 °C, 3 h; (c) Na<sub>2</sub>S<sub>2</sub>O<sub>4</sub> (24 equiv), K<sub>2</sub>CO<sub>3</sub> (30 equiv), paraquat (10 mol%), 1:1 (v/v) CH<sub>2</sub>Cl<sub>2</sub>–water, 40 °C, 4 d; (d) NBS (1.0 equiv), CH<sub>2</sub>Cl<sub>2</sub>, –78 °C, 1 h, **E** (0.12 mmol); (e) NIS (1.0 equiv), 9:1 (v/v) CH<sub>2</sub>Cl<sub>2</sub>–HOAc, r.t., 2 h, **F** (2.61 mmol); (f) mCPBA (2.0 equiv, slow addition), 3:1 (v/v) CH<sub>2</sub>Cl<sub>2</sub>–HOAc, r.t., 1 d, 0.24–11.2 mmol.

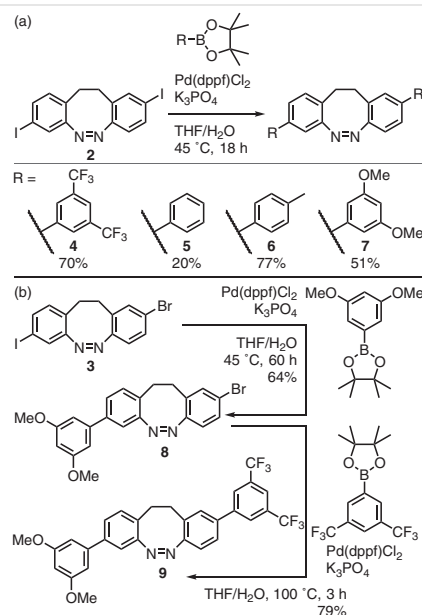
2,8-Pseudo-*para*-halide-substituted diazocines **1**, **2**, and **3** were each synthesized in four steps from commercially available 1,2-bis(2-nitrophenyl)ethane (**D**; Scheme 2). Due to the almost complete electronic decoupling of the two nitrophenyl rings, a selective halogenation of just one of the rings is not possible. Consequently, **D** underwent halogenation with one equivalent of the appropriate *N*-halosuccinimide (NBS or NIS, respectively) in a statistical reaction. This process gave a mixture of nonhalogenated, monohalogenated, and dihalogenated 1,2-bis(2-nitrophenyl)ethanes in approximately a 1:2:1 ratio, which limited the expected yield to a maximum of around 50%. <sup>1</sup>H NMR spectroscopy showed that 52% of the desired isomer **S8** was formed by using NIS. In contrast, the use of NBS resulted in a lower 34% yield of the desired isomer **S1**, because single bromination occurred in both the desired 4-position and the undesired 6-position (SI; Section S3.1). At this stage, separating the isomeric mixture of halogenated dinitro compounds was complex, so it was directly reduced by using sodium dithionite, achieving moderate yields over the two steps.

The reduction conditions varied for the monohalogenated 1,2-bis(2-aminophenyl)ethanes **E** and **F**. Using a 1,4-dioxane–water solvent mixture, sodium dithionite reduction provided good yields of the monobrominated dianiline **E**, achieving a yield of 76% based on the <sup>1</sup>H NMR yield of its nitro counterpart **S1**. In contrast, monoiodinated dianiline **F** only resulted in a yield of 10% (based on the <sup>1</sup>H NMR yield of **S8**; SI, Sections S2.2). We therefore carried out the sodium dithionite reduction of monoiodinated **F** in a biphasic dichloromethane–water mixture using paraquat as an electron-phase-transfer catalyst, achieving a 93% yield (SI, Section S3.2). Isolating dianilines **E** and **F** from their isomers posed challenges; however, their amino groups exhibit increased affinity for silica, aiding this process. Whereas manual column chromatography for purification remained difficult, employing an automated medium-pressure liquid chromatography system gave fast and highly reproducible results (SI, Section S5).

Once the monohalogenated dianilines **E** and **F** had been obtained, they were subjected to a second halogenation step using NBS or NIS. This step resulted in selective halogenation at the *para*-position relative to the amino group on the less substituted aromatic ring, producing good to excellent yields of the dihalogenated dianilines **G**, **H**, and **I** (akin to the method used by Trauner and co-workers)<sup>2</sup> (SI, Sections S2.3–S2.5). In this second halogenation step, the selectivities for NBS and NIS were reversed compared with the first halogenation step. The greater reactivity of NBS facilitated near-quantitative formation of **G** and **I** at –78 °C. In contrast, the less reactive NIS required acid activation at room temperature for adequate conversion, which notably diminished the selectivity toward **H** to 53%. Oxidative ring closure using *meta*-chloroperoxybenzoic acid<sup>2</sup> (mCPBA) of dianilines **G**, **H**, and **I** afforded the corresponding 2,8-pseudo-*para*-halogenated diazocines **1**, **2**, and **3** in good yields.

Our synthetic approach is readily scalable, as was demonstrated by a gram-scale synthesis of the bromo iodo diazocine **3** (SI, Section S4). Although scaling up the halogenation and oxidation steps was straightforward, the biphasic reduction exhibited lower yields at larger scales (93% at 0.4 mmol, 36% at 8 mmol, 12% at 60 mmol). We consider this decreased yield in the initial synthetic step acceptable because of the cheap and easily accessible reagents that are used.

2,8-Pseudo-*para*-halogenated diazocines **1**, **2**, and **3** are excellent platforms for potential functionalization by, for example, C–C,<sup>19–22</sup> C–N,<sup>2,23</sup> or C–S<sup>24</sup> cross-coupling reactions. To demonstrate the exceptional ease with which diazocines **1**, **2**, and **3** can be functionalized through cross-coupling reactions, we subjected diiodo diazocine **2** to Suzuki cross-coupling reactions with various arylboronic acid pinacol esters, thereby incorporating electron-rich or electron-deficient substituents onto the diazocine framework (Scheme 3a). Diazocines **4**–**7**, which incorporate two 3,5-bis(trifluoromethyl)phenyl, two phenyl, two tolyl, and two 3,5-dimethoxyphenyl substituents, respectively, were obtained in moderate to good yields. Crucially, the bromo iodo diazocine **3** permits the highly selective sequential introduction of two different substituents onto the diazocine scaffold, yielding the asymmetrically substituted diazocine **9** (Scheme 3b), which features both an electron-rich and an electron-deficient substituent on one photoswitch.



**Scheme 3** (a) A range of 2,8-pseudo-*para* aryl-substituted diazocines can be obtained from diiodo diazocine **2** through Suzuki cross-coupling reactions. (b) The substituents vary from electron-rich to electron-deficient (left to right). Bromo iodo diazocine **3** permits the selective introduction of two distinct substituents, for example, one electron-rich and one electron-deficient substituent (**9**).

$\text{Pd}(\text{dppf})\text{Cl}_2$  served as a catalyst for all the cross-coupling reactions, as it demonstrated the highest selectivity in producing the brominated (3,5-dimethoxy)phenyldiazocine **8** at 45 °C (SI, Section S3.3).

The photochemical and photophysical properties of diazocines **1–9** were investigated by UV-vis spectroscopy [thermal half-lives ( $\tau_{1/2}$ )] and  $^1\text{H}$  NMR spectroscopy [photostationary states (PSS)] in dichloromethane (Table 1).  $Z \rightarrow E$  and  $E \rightarrow Z$  isomerizations were achieved by irradiating the respective  $n \rightarrow \pi^*$  bands [ $\lambda_{\text{max}}(Z) \approx 400 \text{ nm}$ ;  $\lambda_{\text{max}}(E) \approx 490 \text{ nm}$ ]. Illuminating diazocines **1–9** with 385 nm light for four to five minutes at NMR concentrations induced  $Z \rightarrow E$  conversion, resulting in photostationary states of between 63 and 77%.  $E \rightarrow Z$  isomerization occurred quantitatively under 505 nm light irradiation for one to two minutes or through thermal relaxation, with thermal half-lives ( $\tau_{1/2}$ ) of between 1.4 and 6.1 hours (3.5 h on average). These values are notably lower than those of parent diazocine **A** ( $\tau_{1/2} = 8.0 \text{ h}$ ), a frequent finding for disubstituted diazocines.<sup>2</sup> The photostationary states of the substituted diazocines varied from 63 to 77%. Dibromo, diiodo, and bromo iodo diazocines **1**, **2**, and **3** showed photostationary states that were as much as 14% lower than that of the parent diazocine **A**. Diazocines **4–9** interestingly showed a minor influence of the electron-rich or electron-deficient nature of their substituents on the photostationary states depending on their electronic conjugation with the diazocine phenyl groups. The most significant observed decrease in the photostationary state (14%) was seen with asymmetrically substituted diazocine **9** (compared to **4**), which contained both an electron-deficient and an electron-rich substituent. Although this decline is not negligible, previous observations<sup>2</sup> indicated a 48% reduction in photostationary states when moving from two electron-deficient substituents to a pairing of one electron-rich and one electron-deficient substituent. Thus, the

electronic characteristics of the phenyl substituents have a noticeable, albeit relatively small, effect on the thermal half-lives and photostationary states of the diazocines.

We believe that the torsion between the diazocine phenyls and the phenyl substituents interferes with the electronic conjugation between the electron-withdrawing or -donating groups and the azo-group thereby minimizing the impact of these substituents on the photophysical properties. This is particularly clear when comparing the excellent  $n \rightarrow \pi^*$  band separation in diazocines **1**, **4**, and **7** with that in the parent system **A** (Figure 2), which shows minimal sensitivity to variations in the substituents. Therefore, the bi-phenyl connection presents a viable alternative for introducing methylene or ethylene groups<sup>9,25</sup> to achieve electronic decoupling between diazocines and their substituents.

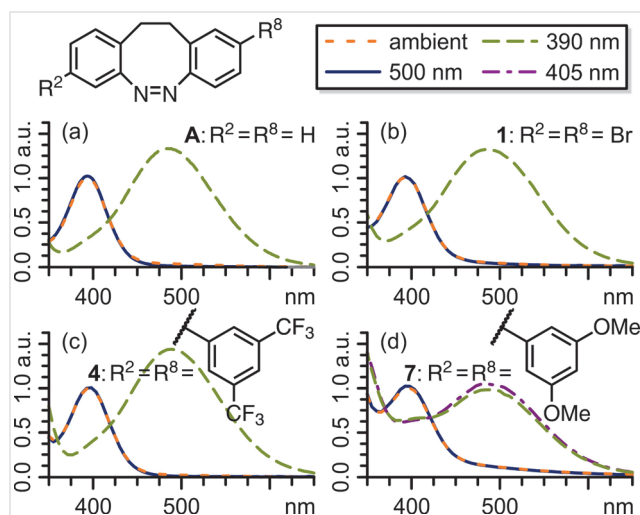


**Figure 2** Normalized UV-vis absorption spectra ( $\text{CH}_2\text{Cl}_2$ , 0.8–1.6 mM, 298 K) of diazocines (a) **A**, (b) **1**, (c) **4**, and (d) **7** under ambient light (orange) and in their respective PSS after 390 nm and 500 nm light irradiation (blue and green, respectively; 405 nm for **7**, purple).

**Table 1** Photostationary States (PSS at 385 and 505 nm, 298 K), Absorption Maxima ( $\lambda_{\text{max}}$ ), and Half-Lives ( $\tau_{1/2}$ ; 298 K) as Determined by  $^1\text{H}$  NMR (PSS) and UV-vis Spectroscopy ( $\lambda_{\text{max}}$ ,  $\tau_{1/2}$ ) in  $\text{CH}_2\text{Cl}_2$

Molecule	PSS <sub>385</sub> (% E)	PSS <sub>505</sub> (% Z)	$\lambda_{\text{max}}(Z)$ (nm)	$\lambda_{\text{max}}(E)$ (nm)	$\tau_{1/2}$ (298 K) (h)
<b>A</b>	87	99	401	490	8.0
<b>1</b>	77	98	400	485	3.5
<b>2</b>	75	>99	400	485	3.2
<b>3</b>	76	>99	400	485	3.7
<b>4</b>	73	97	405	490	4.4
<b>5</b>	73	>99	405	490	3.7
<b>6</b>	66	97	405	490	3.7
<b>7</b>	67	99	405	490	1.4
<b>8</b>	72	>99	400	485	6.1
<b>9</b>	63	98	405	490	2.1

In conclusion, nine asymmetrically pseudo-*para*-substituted diazocines **1–9** have been synthesized and characterized. The synthesis of dihalogenated diazocines **1–3** was achieved in four simple steps that use affordable readily available reagents, and can be scaled up to a minimum of 40 mmol. Various aryl substituents were introduced onto diiodo diazocine **2** to give diazocines **4–7**, showcasing its effective reactivity in cross-coupling reactions. Asymmetric substitution to give diazocines **8** and **9** was selectively accomplished by using the bromo iodo diazocine **3**. Although electronic conjugation exists between the aryl substituents and the diazocine cores, the influence of these substituents' electron-donating or electron-withdrawing characteristics on the photophysical properties of the photoswitches was minimal. The significant structural change that occurs during  $Z \rightarrow E$  isomerization, along with a decreased reliance on substituent effects for photophysical properties, their



ease of synthesis, and their extensive potential for functionalisation through C–X coupling reactions make dihalogenated diazocines **1–3** important future building blocks for photoresponsive polymers used in smart materials, photodynamic therapy, molecular imaging, and optical data storage.

## Conflict of Interest

The authors declare no conflict of interest.

## Author contributions

M.J.N. and L.K.S.v.K. conceptualized the project and all authors were involved in developing the details. M.J.N., V.S., V.P., and J.S.K. synthesized and investigated the compounds. Formal analysis was performed by M.J.N. and V.S. L.K.S.v.K. visualized the data for the manuscript and wrote the original draft. All authors contributed to reviewing and editing the final draft.

## Funding Information

This work was supported by the Fonds der Chemischen Industrie (Liebig Fellowship) and the German Research Foundation (DFG, Emmy Noether Programme, 446317932). M.J.N. and V.S. thank the FCI and Avicenna-Studienwerk, respectively, for their Ph.D. scholarships.

## Supporting Information

Supporting information for this article is available online at <https://doi.org/10.1055/a-2567-1399>.

## References and Notes

- Siewertsen, R.; Neumann, H.; Buchheim-Stehn, B.; Herges, R.; Näther, C.; Renth, F.; Temps, F. *J. Am. Chem. Soc.* **2009**, *131*, 15594.
- Maier, M. S.; Hüll, K.; Reynders, M.; Matsura, B. S.; Leippe, P.; Ko, T.; Schäffer, L.; Trauner, D. *J. Am. Chem. Soc.* **2019**, *141*, 17295.
- Ewert, J.; Heintze, L.; Jordà-Redondo, M.; von Glasenapp, J.-S.; Nonell, S.; Bucher, G.; Peifer, C.; Herges, R. *J. Am. Chem. Soc.* **2022**, *144*, 15059.
- Heintze, L.; Schmidt, D.; Rodat, T.; Witt, L.; Ewert, J.; Kriegs, M.; Herges, R.; Peifer, C. *Int. J. Mol. Sci.* **2020**, *21*, 8961.
- López-Cano, M.; Scortichini, M.; Tosh, D. K.; Salmaso, V.; Ko, T.; Salort, G.; Filgaira, I.; Soler, C.; Trauner, D.; Hernando, J.; Jacobson, K. A.; Ciruela, F. *J. Am. Chem. Soc.* **2025**, *147*, 874.
- Cabré, G.; Garrido-Charles, A.; González-Lafont, A.; Moormann, W.; Langbehn, D.; Egea, D.; Lluch, J. M.; Herges, R.; Alibés, R.; Busqué, F.; Gorostiza, P.; Hernando, J. *Org. Lett.* **2019**, *21*, 3780.
- Li, S.; Han, G.; Zhang, W. *Macromolecules* **2018**, *51*, 4290.
- Burk, M. H.; Langbehn, D.; Hernández Rodríguez, G.; Reichstein, W.; Drewes, J.; Schröder, S.; Rehders, S.; Strunskus, T.; Herges, R.; Faupel, F. *ACS Appl. Polym. Mater.* **2021**, *3*, 1445.
- Li, S.; Bamberg, K.; Lu, Y.; Sönnichsen, F. D.; Staubitz, A. *Polymers* **2023**, *15*, 1306.
- Burk, M. H.; Schröder, S.; Moormann, W.; Langbehn, D.; Strunskus, T.; Rehders, S.; Herges, R.; Faupel, F. *Macromolecules* **2020**, *53*, 1164.
- Wang, Y.; Yuan, Y.; Zhang, S.; Chen, L.; Chen, Y. *Chin. J. Chem.* **2024**, *42*, 3278.
- Li, S.; Colaco, R.; Staubitz, A. *ACS Appl. Polym. Mater.* **2022**, *4*, 6825.
- Bannwarth, C.; Ehlert, S.; Grimme, S. *J. Chem. Theory Comput.* **2019**, *15*, 1652.
- Okada, T.; Sugihara, M.; Bondar, A.-N.; Elstner, M.; Entel, P.; Buss, V. *J. Mol. Biol.* **2004**, *342*, 571.
- Choe, H.-W.; Kim, Y. J.; Park, J. H.; Morizumi, T.; Pai, E. F.; Krauß, N.; Hofmann, K. P.; Scheerer, P.; Ernst, O. P. *Nature* **2011**, *471*, 651.
- Löw, R.; Rusch, T.; Röhricht, F.; Magnussen, O.; Herges, R. *Beilstein J. Org. Chem.* **2019**, *15*, 1485.
- Bastien, G.; Severa, L.; Škuta, M.; Santos Hurtado, C.; Rybáček, J.; Šolínová, V.; Čísařová, I.; Kašička, V.; Kaleta, J. *Chem. Eur. J.* **2024**, *30*, e202401889.
- Li, S.; Eleya, N.; Staubitz, A. *Org. Lett.* **2020**, *22*, 1624.
- Hugenbusch, D.; Lehr, M.; von Glasenapp, J.-S.; McConnell, A. J.; Herges, R. *Angew. Chem. Int. Ed.* **2023**, *62*, e202212571.
- Zheng, T.; Tan, L.; Lee, M.; Li, Y.; Sim, E.; Lee, M. *J. Am. Chem. Soc.* **2024**, *146*, 25451.
- Schultzke, S.; Walther, M.; Staubitz, A. *Molecules* **2021**, *26*, 3916.
- Lee, H.; Tessarolo, J.; Langbehn, D.; Baksi, A.; Herges, R.; Clever, G. H. *J. Am. Chem. Soc.* **2022**, *144*, 3099.
- Deng, J.; Wu, X.; Guo, G.; Zhao, X.; Yu, Z. *Org. Biomol. Chem.* **2020**, *18*, 5602.
- Berry, J.; Lindhorst, T. K.; Despras, G. *Chem. Eur. J.* **2022**, *28*, e202200354.
- Moormann, W.; Langbehn, D.; Herges, R. *Beilstein J. Org. Chem.* **2019**, *15*, 727.
- 2-Bromo-8-iodo-11,12-dihydrodibenzo[c,g][1,2]diazocine (3)**  
A solution of *m*CPBA (75%, 2.58 g, 11.22 mmol, 2.00 equiv) in glacial HOAc (~0.6 M) was added to a solution of bromo iodo dianiline **1** (2.34 g, 5.61 mmol, 1.00 equiv) in 1:3 glacial HOAc–CH<sub>2</sub>Cl<sub>2</sub> (60 mL) over 24 hours using a syringe pump. The mixture was then stirred for 18 h at r.t., then neutralized with sat. aq NaHCO<sub>3</sub>. The organic layer was separated, washed with sat. aq NaHCO<sub>3</sub> (25 mL) and sat. aq NaCl (25 mL), dried (MgSO<sub>4</sub>), and concentrated by rotary evaporation. The residue was purified by column chromatography [silica gel, cyclohexane–EtOAc (100:0 to 70:30 over 15 column volumes)] to give a yellow solid; yield: 1.47 g (63%, 3.56 mmol). *R*<sub>f</sub> = 0.56 (cyclohexane–EtOAc, 8:2).  
<sup>1</sup>H NMR (500 MHz, CD<sub>2</sub>Cl<sub>2</sub>): δ = 2.64–2.96 (m, 4 H, H-7, H-8), 6.74 (d, *J* = 8.3 Hz, 1 H, H-11), 6.78 (d, *J* = 8.1 Hz, 1 H, H-5), 7.16 (d, *J* = 1.8, 1 H, H-2), 7.18 (d, *J* = 2.1 Hz, 1 H, H-14), 7.31 (dd, *J* = 8.4 Hz, 2.1, 1 H, H-12), 7.39 (dd, *J* = 8.1, 1.8 Hz, 1 H, H-4). <sup>13</sup>C NMR (126 MHz, CD<sub>2</sub>Cl<sub>2</sub>): δ = 31.0 (C-7), 31.1 (C-8), 90.9 (C-3), 120.3 (C-13), 120.6 (C-11), 127.2 (C-2), 127.7 (C-6), 129.9 (C-12), 130.2 (C-9), 131.6 (C-15), 132.4 (C-14), 136.1 (C-4), 154.1 (C-10), 156.2 (C-1). HRMS (ESI<sup>+</sup> Orbitrap): *m/z* [M + H]<sup>+</sup> calcd for C<sub>14</sub>H<sub>15</sub>BrIN<sub>2</sub> = 412.9145; found: 412.9138.